



# High spatiotemporal resolution traffic CO<sub>2</sub> emission maps derived from Floating Car Data (FCD) for 20 European cities (2023)

Qinren Shi<sup>1</sup>, Philippe Ciais<sup>1</sup>, Nicolas Megel<sup>2</sup>, Xavier Bonnemaizon<sup>1</sup>, Rohith Teja Mittakola<sup>1</sup>, Richard Engelen<sup>3</sup>, Chuanlong Zhou<sup>1</sup>

<sup>1</sup>Le Laboratoire des Sciences du Climat et de l'Environnement, Saint-Aubin, 91190, France

<sup>2</sup>NEXQT SAS, Paris, France

<sup>3</sup>ECMWF, Robert-Schuman-Platz 3, 53175 Bonn, Germany

*Correspondence to:* Qinren Shi([qinrenshi2025@gmail.com](mailto:qinrenshi2025@gmail.com)) & Chuanlong Zhou([chuanlong.zhou@lsce.ipsl.fr](mailto:chuanlong.zhou@lsce.ipsl.fr))

**Abstract.** On-road transportation is a major contributor to CO<sub>2</sub> emissions in cities, and high-resolution CO<sub>2</sub> traffic emission maps are essential for analyzing emission patterns and characteristics. In this study, we developed new hourly CO<sub>2</sub> emission maps at 100 × 100 m resolution for 20 major cities in France, Germany, and the Netherlands in 2023. We used commercial Floating Car Data (FCD) based on anonymized GPS signals periodically reported by individual vehicles, providing hourly information on mean speed and on the number of GPS sample counts per street. Machine learning models were developed to fill FCD data gaps and convert sample counts into actual traffic volumes, and the COPERT model was used to estimate speed- and vehicle type dependent emission factors. Hourly emissions, initially estimated at the street level, were aggregated to 100 × 100 m grid cells. Annual on-road CO<sub>2</sub> emissions across the 20 European cities in 2023 ranged from 0.4 to 7.9 Mt CO<sub>2</sub>, with emissions strongly correlated with urban area ( $R^2 = 0.98$ ) and, to a lesser extent, population size ( $R^2 = 0.74$ ). Spatially, emissions are either highly concentrated along major highways in cities such as Paris and Amsterdam or more evenly distributed in cities such as Berlin and Bordeaux, highlighting the need for context-specific mitigation strategies. Temporally, this study shows the CO<sub>2</sub> emission fluctuations due to holiday periods, weekly activity cycles, and distinct usage profiles of different vehicle types. Due to the low latency of FCD, this approach could support near-real-time traffic emission mapping in the future. Our approach enhances the spatial and temporal characterization of CO<sub>2</sub> emissions in on-road transportation compared to the conventional method used in gridded inventories, indicating the potential of FCD data for near-real-time urban emission monitoring and timely policy making. The datasets generated by this study are available on Zenodo <https://doi.org/10.5281/zenodo.16600210>(Shi et al., 2025).



## 31 1 Introduction

32 The road transport sector is one of the largest sources of greenhouse gas (GHG) emissions in the European Union and the only  
 33 major economic sector where carbon dioxide (CO<sub>2</sub>) emissions have risen since 1990, primarily due to the widespread use of  
 34 fossil fuel-powered passenger cars and freight vehicles. In 2023, it accounts for approximately 26.0% of total EU GHG  
 35 emissions (EEA, 2024a). In response to the dual challenge of reducing emissions and developing cleaner mobility  
 36 infrastructures, the European Strategy for Low-Emission Mobility outlines three elements: (1) Increasing the efficiency of the  
 37 transport system, including the optimization of logistics and intelligent transport systems; (2) Accelerating the deployment of  
 38 low-emission alternative energy sources, such as biofuels, renewable electricity, and hydrogen; and (3) Speeding up the  
 39 transition to zero-emission vehicles, through regulatory incentives, infrastructure investment, and innovation support  
 40 (European Commission, 2016). This transition is not only critical for achieving the EU's climate neutrality goal, which  
 41 involves reducing net CO<sub>2</sub> emissions to zero by 2050 (EEA, 2024b), but also for improving air quality, reducing energy  
 42 dependence on fossil fuel imports, and enhancing the competitiveness of European industry.

43  
 44 Emission reduction targets are being translated into concrete actions at the city level. For instance, Paris plans to reduce its  
 45 direct emissions by 50% by 2030 and 100% by 2050, compared to 2004. The transport sector, responsible for approximately  
 46 20% of Paris' local greenhouse gas emissions (Albarus et al., 2025). Paris has set itself the target of phasing out diesel-powered  
 47 mobility by 2024 and petrol-powered mobility by 2030, aligning with the EU-wide ban on the sale of internal combustion  
 48 engine vehicles by 2035. In addition, the city is developing financial incentives and support measures for low-carbon mobility.  
 49 It is also preparing a low-carbon urban logistics plan for the Paris region between now and 2030 (UNFCCC, 2023). Amsterdam  
 50 aims to achieve zero-emission transport by 2030, phasing out all fossil-fuel vehicles within city limits (Amsterdam, 2024). The  
 51 city is rapidly expanding its electric vehicle infrastructure, as all newly registered vehicles are required to have zero-emission  
 52 engines in 2025 (CINEA, 2025). Over 70% of trips are already made by walking, cycling, or public transport, making  
 53 Amsterdam a leader in sustainable urban mobility. Similarly, to achieve climate neutrality in 2050, Berlin will require a long-  
 54 term reduction in CO<sub>2</sub> emissions in the transport sector to around 1.17 million tonnes of CO<sub>2</sub> per year, a reduction of around  
 55 77 % compared with 1990 emissions (diBEK, 2025).

56  
 57 High-resolution emission maps are crucial for monitoring emission changes and providing insights into the effectiveness of  
 58 traffic mitigation policies in cities. For example, a high-resolution (1 km<sup>2</sup>) CO<sub>2</sub> emissions inventory for U.S. road transportation  
 59 named DARTE enables detailed analysis at the city scale between 1980 to 2012 (Gately et al., 2015), revealing that urban areas  
 60 drive most of the emission growth and that traditional population-based downscaling methods substantially misrepresent city-  
 61 level spatial patterns. Over the past decade, several efforts have been made to improve either the temporal or the spatial  
 62 resolution of traffic emission inventories, primarily by incorporating real-world traffic data generated from sensors or GPS  
 63 signals. From a temporal resolution perspective, annual aggregated statistics make it impossible to capture short-term



variations due to weather, policy changes, or special events. Therefore, daily or hourly data were increasingly applied to improve the accuracy. For example, TomTom collects all the travel times and compares them with the lowest travel times to calculate congestion indexes based on FCD(index, 2024). Tomtom congestion indexes were used by Carbon Monitor Cities (Huo et al., 2022) to estimate daily CO<sub>2</sub> emissions for 1500 cities. CAMS-TEMPO is a dataset of European emission temporal profiles that provides gridded monthly, daily, weekly, and hourly weight factors for atmospheric chemistry modelling, and the European part used hourly traffic data collected from over 20 European cities via open-data portals or personal communications (Guevara et al., 2021). One-month GPS-based datasets covering 52,834 conventional fuel vehicles registered in the province of Modena and 40,459 vehicles registered in the province of Firenze were used to generate high-resolution emission maps(De Gennaro et al., 2016). A near-real-time on-road traffic emission product on 2860 km of the main roads in Bangkok was automatically generated by retrieving the traffic data from the Google Maps API service and the Python code every 15 min (Naiudomthum et al., 2022). In recent years, machine learning-based bottom-up approaches have supported the development of high-resolution emission maps. For instance, an hourly street-level emission map of Chengdu was developed using data from 1,454 camera-based sensors and 34 highway monitoring sites, employing land-use random forest models(Wen et al., 2022). Similarly, a platform tracking hourly CO<sub>2</sub> emissions at a 30×30 m resolution was designed for Berlin based on local traffic data, using machine learning methods(Anjos and Meier, 2025).

Despite recent advancements, most city-level emission datasets still suffer from limitations in either temporal or spatial resolution, with few achieving both simultaneously. CAMS-TEMPO(Guevara et al., 2021) and Carbon Monitor(Huo et al., 2022) lack road-specific information and provide only outputs at 0.1° resolution and the city level, respectively. The hourly street-level emission datasets for Chengdu(Wen et al., 2022) and Bangkok(Naiudomthum et al., 2022) only cover one to two months. The Berlin platform offers high spatial and temporal resolution from 2015 to 2022, but may miss data from smaller roads, as counting stations are usually located on major roads.

As part of the Copernicus Atmosphere Monitoring Service (CAMS), this study estimates for the first time hourly street-level on-road transportation CO<sub>2</sub> emissions, aggregated into 100 m resolution hourly maps for 20 European cities in 2023. Hourly GPS-based data, reporting traffic counts and speeds of individual vehicles across different road classes, were upscaled using machine learning to reconstruct complete traffic volumes and speeds across the road networks. Then, CO<sub>2</sub> emissions were estimated using the COPERT model, and emission maps were developed. This approach enhances the spatial and temporal characterization of CO<sub>2</sub> emissions in on-road transportation compared to the downscaling method used in other inventories, indicating the potential of GPS-based data for supporting future efforts in emission monitoring and developing emission reduction policies.



## 2 Data and Method

### 2.1 Overview of the Methodology

Figure 1 describes the methodology of this study. The GPS-based high-resolution ‘Floating Car Data’ (FCD) on individual vehicle flow (GPS vehicles counts per street each hour) and speed covering every street was obtained from a data aggregation provider that collects GPS position data from cars (passenger cars) and trucks (light commercial vehicles and heavy duty trucks), providing road-specific information on hourly average speed and sample counts (i.e., the number of cars recorded in each street for each hour). Those GPS data are linked with precise cities’ road network datasets, providing detailed information on road length, road functional class, and truck access authorization. All data is anonymized by the data provider to prevent compromising any individual or organizational data privacy issues. After raw data processing and cleaning, a machine learning model was used to fill in missing values in FCD, as well as to transform FCD sample counts limited to vehicles equipped with GPS into traffic volumes for all vehicles. Then, the COPERT model (Ntziachristos et al., 2009), the EU standard vehicle emissions calculator, was applied for estimating specific CO<sub>2</sub> emission factors based on individual vehicle hourly average speed and type. Combined with the road lengths obtained from geographical databases and with fleet structures, we finally estimate street-level road-specific emissions using the following equation:

$$Emis_{t,v,r} = N_{t,r} \times Structure_v \times Length_r \times EF_{v,s} \quad (1)$$

Where  $Emis_{t,v,r}$  represents CO<sub>2</sub> emission at the hour  $t$ , for the vehicle type  $v$ , on road  $r$ .  $N_{t,r}$  represents the total traffic volume at hour  $t$ , on road  $r$  (counts/hour).  $Structure_v$  represents the proportion of vehicle type  $v$  in the vehicle fleet (%).  $Length_r$  represents the road length (km) of the road  $r$ , and  $EF_{v,s}$  (g CO<sub>2</sub>/km) represents the CO<sub>2</sub> emission factors for the vehicle type  $v$ , at the hourly average speed  $s$  (km/h).

Our FCD source covers France, Germany, and the Netherlands. Therefore, the 20 most populous cities within these three countries were selected to develop high-resolution emission maps. Table 1 shows the basic information (population, area, street length, street density) of the 20 cities in 2023. Note that here Paris is the administrative city jurisdiction (Ville de Paris) covering the central 20 arrondissements, so its area is much smaller than Berlin, which is both a city and a federal state.

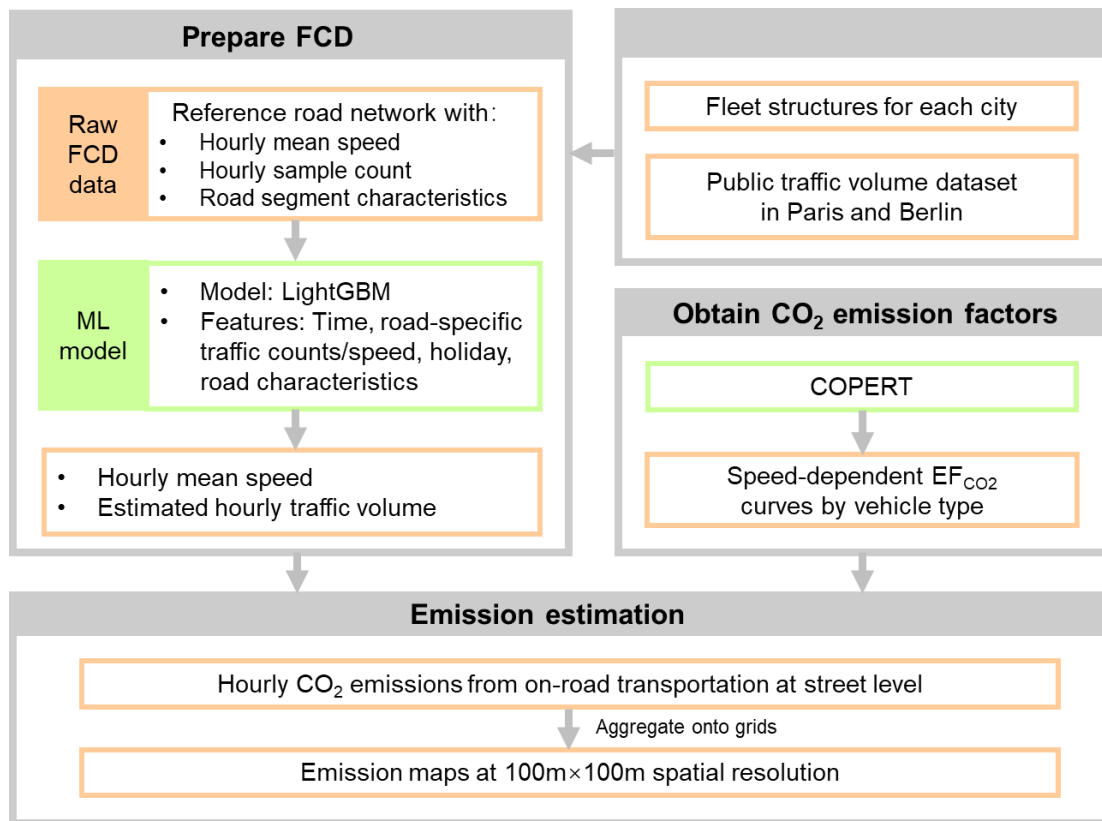


Figure 1: The roadmap of this study



136 **Table 1: Information of 20 selected cities in 2023.**

Country	City	Population (Thousand)	Area(km <sup>2</sup> )	Street length(km)	Street density(km/km <sup>2</sup> )
France	Paris	2,103	105.4	2412.9	22.9
	Marseille	862	240.6	3301.7	13.7
	Lyon	513	47.9	985.3	20.6
	Lille	233	39.5	679.8	17.2
	Toulouse	472	118.3	2311.2	19.5
	Nice	343	71.9	1228.0	17.1
	Nantes	303	65.2	1249.4	19.2
	Strasbourg	277	78.3	1252.4	16.0
	Montpellier	278	56.9	1260.1	22.1
	Bordeaux	250	49.4	967.9	19.6
Germany	Berlin	3,782	891.3	12073.4	13.5
	Hamburg	1,910	755.2	8725.2	11.6
	Munich	1,510	310.7	5220.0	16.8
	Cologne	1,087	405.2	5508.8	13.6
	Frankfurt	776	248.3	3648.5	14.7
	Stuttgart	633	207.3	3660.8	17.7
	Dusseldorf	631	217.4	2741.5	12.6
Netherland	Amsterdam	883	219.4	3203.8	14.6
	Rotterdam	656	324.1	3555.7	11.0
	The Hague	553	98.1	1796.8	18.3

137

138 **2.2 Description and preparation of FCD**

139 FCD provides hourly average speed and sample counts for each street, with separate data for cars and trucks reporting GPS  
140 data. The FCD is linked with high-resolution road network datasets that feature information such as road length, speed category,



road functional class, lane category, on more detailed and complete road networks than public traffic datasets based on sensors. As shown in Figure 2, public datasets used by previous studies are only available for a few cities and provide hourly traffic data for 3,739 road segments in Paris (Xavier Bonnamaizon 2024) and 19,808 segments in Berlin (Anjos and Meier, 2025), respectively. In contrast, FCD gives vehicle count samples and speed information for 36,716 roads in Paris and 122,759 roads in Berlin, dividing long roads into more segments and encompassing a much greater number of small roads than the city-level public datasets. All road segments were categorized into major, middle, and small according to the functional class defined by the FCD. Major roads represent roads connecting major metropolitan areas, middle roads represent roads connecting neighbourhoods, and small roads represent low-volume roads.

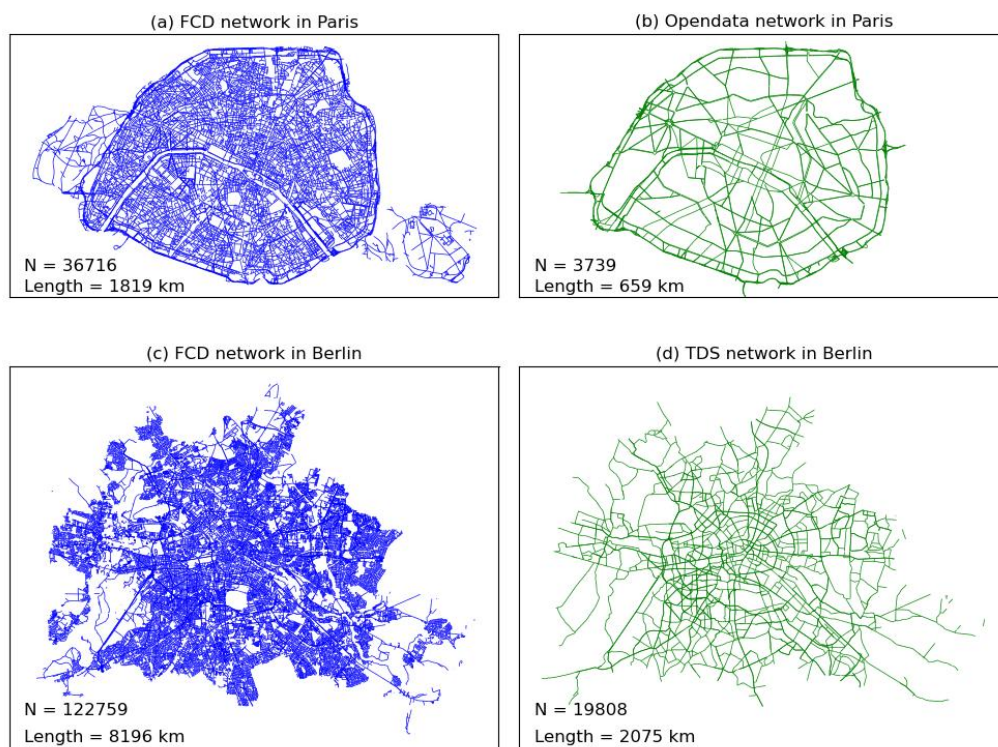


**Figure 2: Monitored road networks in this study and other public datasets in Paris and Berlin.** N represents the number of road segments. (a) and (c) represent road networks from FCD for Paris and Berlin, respectively; (b) and (d) represent networks from Open Data in Paris and Traffic Detection Systems in Berlin.

Missing values exist in the FCD due to unstable GPS signals, especially for small roads. The average data coverage of GPS cars on major, middle, and small roads ranges from 67.0% - 97.7%, 40.4% - 93.8%, and 6.1% - 37.7%, respectively (Figure S1a). The average data coverage of trucks is lower, ranging from 32.2% - 75.8%, 32.1% - 85.3%, and 1.8% - 32.2%, respectively (Figure S1b). Machine learning was used here to fill data gaps, as the use of machine learning techniques has shown great potential for both temporal and spatial imputation of missing data to reconstruct the full volume of traffic(Wen et





al., 2022). Eight features were chosen as predictors (Table 2) to train models. Temporal features (hour, day of the week, and month) were used to capture diurnal and seasonal patterns in traffic behaviour. Observed road-specific daily mean traffic counts and speeds were also used as indicators of baseline traffic intensity. Holiday indicators, including school and public holidays, were included to account for potential shifts in travel demand. Finally, road characteristics including speed category, functional class, and lane category were used to describe the physical and functional attributes of each road segment.

**Table 2: Spatial-temporal features used as predictors of traffic variables**

Category	Features	Usage
Time	Hour, Day of week, Month	Diel and seasonal pattern
Road-specific traffic counts/speed	Daily mean	Baseline traffic intensity
Holiday	School holiday, Public holiday	Potential shifts in travel demand
Road characteristics	Speed category, Functional class, Lane category	Road capacity and flow characteristics

The full-year dataset was partitioned into two temporally isolated subsets: January-June (H1) and July-December (H2) due to the large-scale dataset. Separate machine learning models were developed for each six-month interval, both incorporating consistent feature engineering protocols for vehicle type differentiation (Cars and Trucks) and road classification. Model training was conducted on 80% of the available data, with the remaining 20% held out as an independent test set to evaluate generalization performance. Random forest (RF) and lightGBM models were tested for Paris to compare their performances. As shown in Table S1, Random Forest (RF) and LightGBM exhibited comparable predictive performance across different vehicle types, road types, and target variables (i.e., vehicle count and speed) but LightGBM required significantly less computational time. In some cases, the efficiency gain is more than 10-fold e.g., to fill gaps of car count on major roads takes





6.25 s for LightGBM vs. 122.53 s for RF. This efficiency gains stems from LightGBM's histogram-based decision tree learning and its leaf-wise tree growth strategy with depth constraints, which together enable faster training and better scalability, especially for large datasets with continuous features. Given its high accuracy and computational efficiency, we selected LightGBM was chosen as the preferred model and trained individually for each of the 20 cities.

The LightGBM validation results are shown in Table S2. Overall, the model demonstrates strong predictive performance across different vehicle types and target variables. For car count, performance is consistently high on major roads, with  $R^2$  values typically above 0.90 and reaching up to 0.97 (e.g., The Hague and Amsterdam). On middle and small roads,  $R^2$  varies between 0.53 and 0.85, and lower values are often observed in cities with smaller datasets, such as Lyon and Nice, suggesting that data volume plays a critical role in model accuracy (Figure S2). For car speed, the model also performs well on major roads  $R^2$  (0.85-0.95) but shows greater variability on smaller roads, where  $R^2$  drops to as low as 0.39 in some cases (e.g., Paris or Lyon). The results of trucks are similar to those of cars, but with slightly lower overall performance. Shapley values, a concept from cooperative game theory, are widely used to explain feature importance in machine learning. This study used the Python package SHAP to estimate Shapley values applied to the model's conditional expectation function (SHAP, 2025), revealing that the daily mean count and hour of day are the most influential predictors, followed by day of week, road class, and month (Figure S3). High traffic volumes are associated with increased model output, while hourly effects vary by time of day. In contrast, features such as lane type and school holidays show limited influence.

## 2.2 Obtain CO<sub>2</sub> emission factors using COPERT

To calculate the speed-dependent emission factors  $EF_{CO_2}$  defined by CO<sub>2</sub> emissions per km driven for each vehicle type, we applied the COPERT model, a widely used emissions calculator for vehicles in Europe (Ntziachristos et al., 2009). Monthly temperature and relative humidity data required as input for COPERT were obtained from ERA5 reanalysis (Hersbach, 2023) and interpolated to a 0.01° spatial resolution. City-level averages of maximum/minimum temperature and relative humidity were then calculated within administrative boundaries defined by Eurostat shapefiles to serve as inputs for COPERT.<sup>5</sup> Considering the data scale and time cost, instead of running COPERT for each street segment each hour, this study developed fitting curves between speed and  $EF_{CO_2}$  to obtain  $EF_{CO_2}$ . Except for L-Category vehicles running on diesel, where COPERT provides a fixed value, emission factors were simulated for various vehicle types at speeds of 20, 40, 60, 80, 100, 120, and 140 km/h. Then, for each city, cubic functions were fitted to COPERT simulations, as given by:

$$EF = a \times s^3 + b \times s^2 + c \times s + d \quad (2)$$

Where  $s$  represents the average speed at hourly resolution, and  $a$ ,  $b$ ,  $c$ , and  $d$  are city-specific constants. Table S3 presents the parameters of the curve fitting results for all cities, showing a good fit quality with an  $R^2$  value range from 0.882 to 0.998. In this way, the corresponding emission factor for any given speed can be determined. Note that we used  $EF_{CO_2}$  of the EU6



standard, since CO<sub>2</sub> emission factors are only marginally influenced by emission standards, and this approach was also adopted by TomTom (Index, 2024).

## 2.3 Estimate real traffic volume from sample count

Road-specific hourly total traffic volume is the key parameter to estimate CO<sub>2</sub> emissions. Since not all vehicles transmit GPS signals and our dataset only captures a subset of the real GPS data for all vehicles, the actual traffic volume is significantly higher than the sample counts from the FCD. To solve this problem, we established a relationship between real traffic volume data and GPS sample count using machine learning. Due to the availability of traffic volume data, only the Opendata from Paris (Parisopendata, 2024) and Traffic detection Berlin (Berlinopendata, 2024) were used for modelling. Opendata from Paris provides hourly total vehicle flow from permanent sensors with electromagnetic loops on 2086 roads in 2023, but does not differentiate between vehicle types for the traffic volume. Therefore, the numbers of cars and trucks are estimated based on the proportion of sample counts from each type in our FCD. Traffic detection in Berlin provides hourly total vehicle volumes on 19808 roads, and only the volumes of cars were used for modelling. As shown in Figure 2, monitored road networks of public datasets and FCD are different. The overlap rate and angle are used as criteria to link the two datasets' shapefiles (Figure S4). When the overlap rate > 0.7 and the angle < 20°, a road is identified as being the same in Opendata and FCD. In this way, hourly open data from 3,018 monitoring sites in Paris and 202 in Berlin were matched to the FCD, and we got the real volume and the number of FCD sample counts on the same road. A similar set of predictors as listed in Table 2, except for road-specific traffic counts and speeds, was used to build a LightGBM model to extrapolate FCD sample counts to total traffic volume. For cars in German cities, we used the LightGBM model trained on Berlin's data, while for all other cities, we used the LightGBM trained on Paris's data. The results of validation are shown in Table S4. The validation results (Table S4) show that the LightGBM model performs well on major roads in both Paris ( $R^2 = 0.91$  for cars and 0.88 for trucks) and Berlin ( $R^2 = 0.66$  for cars). The accuracy decreases on middle and small roads in Paris ( $R^2$  range from 0.22 to 0.38), while the performance in Berlin remains comparatively good ( $R^2$  range from 0.86 to 0.88).

## 2.4 Fleet structure

This study collected fleet structures data in 2023 for the 20 cities to further map cars and trucks to 5 categories (passenger cars, light commercial vehicles, buses, L-category and heavy-duty trucks), and 12 sub-categories, 10 fuels (petrol, diesel, CNG, diesel hybrid, biodiesel, diesel PHEV, CNG biofuel, petrol hybrid, battery electric) (Table S5). The data was collected from the official statistical websites of France, Germany, and the Netherlands (Table S6). Only direct emissions from fossil fuels are considered, so the emission factor of battery electric cars is set to 0.



## 2.5 Aggregation onto grids

Python was used to map street network emissions data onto a  $100 \times 100$  m grid. Starting from a shapefile containing road segments with associated emissions, a spatial join was performed using GeoPandas' sjoin function to identify which road segments intersect each grid cell. Emissions were then allocated to the grid cells in a length-weighted manner, proportionally distributing each road segment's emissions based on the length of its overlap with each cell. For the projections, cities in France use EPSG:2154, while most German cities use EPSG:25832; Berlin uses EPSG:25833 due to its location. Dutch cities are projected using EPSG:28992.

## 3 Results

### 3.1 Annual emissions

The total on-road CO<sub>2</sub> emissions in 2023 among the 20 cities ranged from 0.4 Mt CO<sub>2</sub>/yr to 7.9 Mt CO<sub>2</sub>/yr. The top five emitting cities are Berlin (7.9 Mt), Hamburg (6.6 Mt), Cologne (4.1 Mt), Munich (3.5 Mt), and Rotterdam (3.0 Mt). Berlin's CO<sub>2</sub> emissions are approximately 20 times higher than those of Lille, the city with the lowest emissions in the dataset (0.4 Mt). On average, the 20 cities emit 2.4 Mt CO<sub>2</sub> per year, with a coefficient of variation of 0.82 (Figure 3a). As shown in Figure 4, the linear regression analyses between on-road CO<sub>2</sub> emissions and both urban area and population indicate strong positive relationships. Specifically, CO<sub>2</sub> emissions increase significantly with larger urban areas and higher population sizes. The regression model yields a high coefficient of determination with an R<sup>2</sup> value of 0.98 when emissions are regressed against area, suggesting that urban land extent is a dominant factor influencing total emissions. A similarly positive but weaker correlation is observed between emissions and population, with an R<sup>2</sup> value of 0.74, indicating that population size also plays a substantial role in shaping emission levels. This distinction is further illustrated by a comparison between Paris and Hamburg. While their populations are relatively similar, Hamburg covers an urban area nearly seven times larger than that of central Paris. Furthermore, Hamburg's road network is more than three times as long. As a result, Hamburg exhibits substantially higher on-road CO<sub>2</sub> emissions, reinforcing the observation that urban spatial extent and infrastructure scale are critical determinants of total emissions, potentially more so than population alone.

Per capita emissions show a mean of 2.8 tons/person with a coefficient of variation of 0.4, and the ranking is quite different from total emissions (Figure 3b). Some of the cities with high total emissions also have high per capita emissions, such as Cologne (3.8 t/person), Rotterdam (4.6 tons/person) and Frankfurt (3.6 tons/person). Other cities like Berlin (2.1 t/person) and Paris (0.9 t/person) exhibit low per capita values despite their large total emissions. Notably, cities such as Toulouse (3.4 tons/person) and Marseille (3.2 tons/person) have high per capita emissions, highlighting differences in cities' boundaries e.g., including or not satellite towns commuting with each 'city', transportation infrastructure, commuting patterns, and vehicle efficiency across the regions. Figure 3c illustrates the emissions per unit area, revealing a contrasting pattern to total emissions.



Paris exhibits the highest emissions per unit area ( $0.02 \text{ Mt/km}^2$ ), despite having one of the lowest per capita values, which is indicative of its dense urban environment and intensive transportation activities within a compact city layout and a very dense street network. Similarly, Toulouse ranks second in per-area emissions, despite being only seventh in total emissions. This result shows that urban density and mobility intensity significantly influence emission distribution at the local scale.

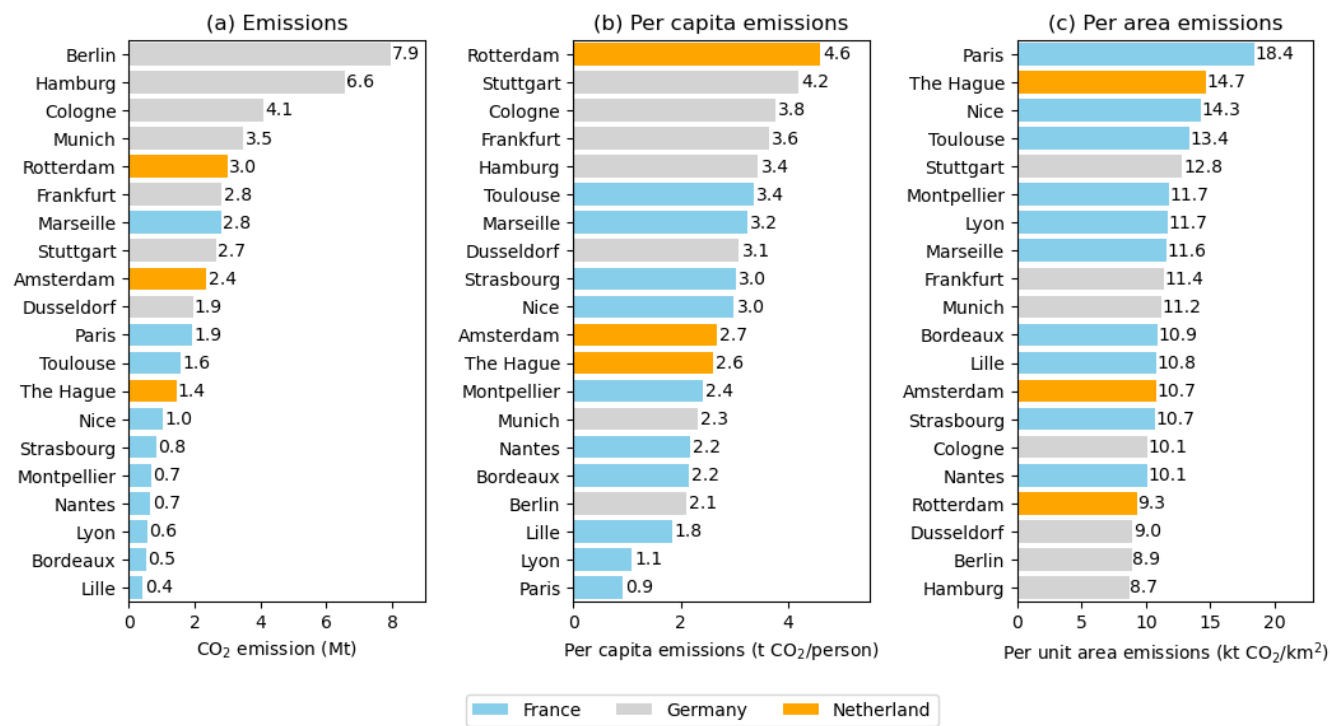


**Figure 3: Annual CO<sub>2</sub> emission and emission intensities per capita and per unit area of 20 cities in 2023.** Grey, light blue and orange represent cities in Germany, France and the Netherlands, respectively.

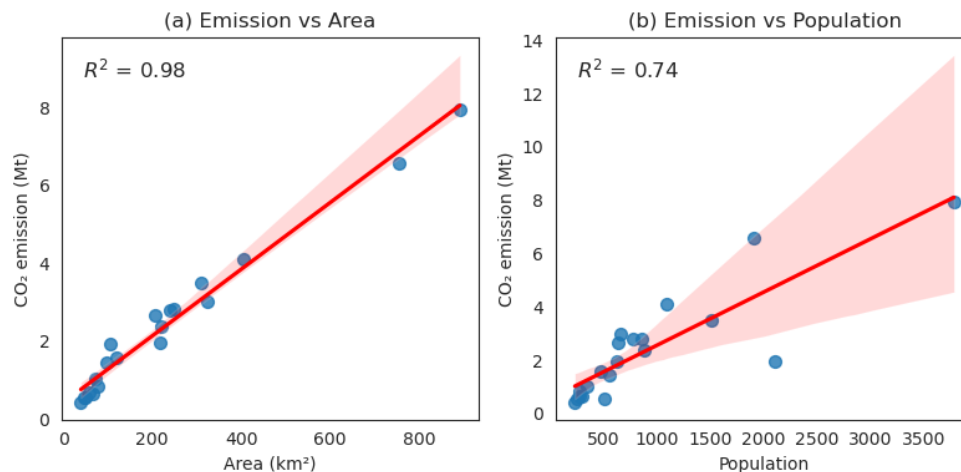


**Figure 4: Linear relationships between on-road CO<sub>2</sub> emissions, area, and population. Each point represents one city.**

### 3.2 Spatial patterns

Figure 5 presents the annual emission maps for 20 major European cities, highlighting the diversity in emission spatial patterns. In addition, two cities from each country were selected to plot cumulative emission curves, as shown in Figure S5. In cities such as Paris, Amsterdam, The Hague and Dusseldorf, a few major roadways stand out significantly in bright yellow. In Paris, the top 5% of the highest-emitting 100 m grids contribute 33.1% of total emissions. The ring road known as le Périphérique emerges as a major hotspot, accounting for 26.9% of the city's total on-road emissions and having a mean emission level that is 953.3% higher than the city-wide average. This is primarily attributable to its high traffic density and heavy vehicle usage driven by significant commuter flows. A similar concentration of emissions is observed in Amsterdam, where the top 5% of the highest-emitting 100 m grids contribute 30.3% of total emissions, respectively, underscoring the spatially skewed distribution of traffic-related CO<sub>2</sub>. The top 5% of high-emission grids in The Hague and Dusseldorf show a lower contribution of total emissions (24.5% and 21.9% respectively), but these are still concentrated along major highways such as the A4 and A12 in the Hague and B8 and A44 in Dusseldorf. The steep curvatures at the start of the cumulative emissions distribution curves for these two cities suggest that only a few key segments are disproportionately responsible for emissions, albeit to a lesser extent than in Paris or Amsterdam.

Cities like Berlin and Bordeaux exhibit a more diffuse emission pattern, with relatively less pronounced hotspots, where the top 5% of the highest-emitting 100 m grids contribute ~19.0% of total emissions. Their cumulative emission curves demonstrate gentler slopes, indicating a more uniform spread of emissions across the road network. This suggests that no single road or corridor dominates in terms of emission contributions and that urban transport emissions are more evenly distributed. Other cities, including Lyon, Marseille, Frankfurt, and Rotterdam, fall between these two extremes, exhibiting



300 varying degrees of emission concentration. For instance, Frankfurt shows notable linear patterns corresponding to high-  
301 emission highways intersecting the urban core. In contrast, Rotterdam reveals both concentrated and dispersed emission zones  
302 due to its mixed land use and logistic traffic. Overall, these spatial variations emphasize the importance of city-specific  
303 mitigation strategies. While targeted interventions on a few high-emitting corridors may yield significant benefits in cities with  
304 highly skewed distributions (e.g., Paris or Dusseldorf), broader, network-wide policies may be necessary in more evenly  
305 distributed urban contexts like Berlin or Bordeaux.

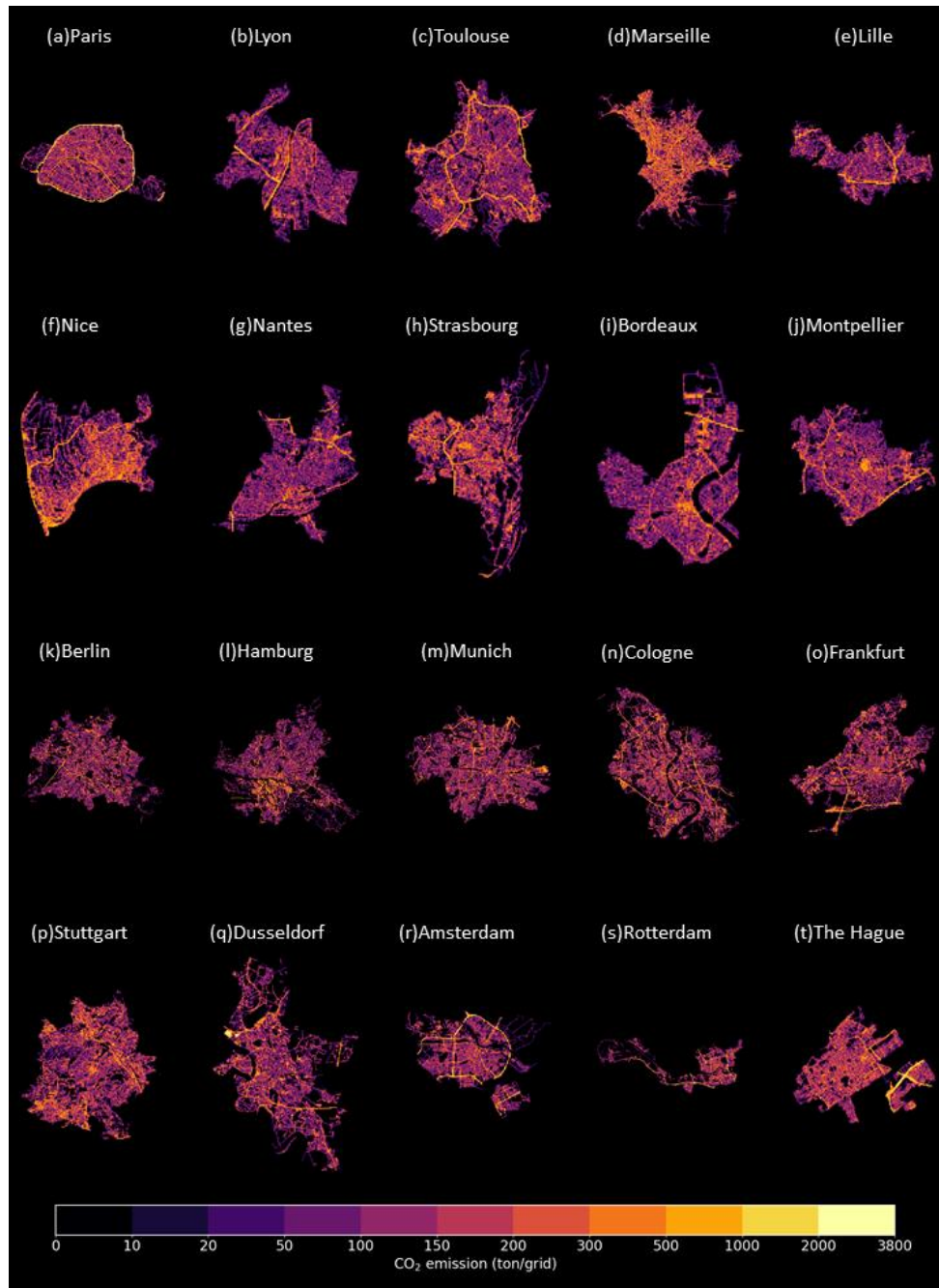


Figure 5: Annual CO<sub>2</sub> emission map of 20 cities at 100m × 100m resolution in 2023.





### 3.3 Temporal patterns

Figure 6 presents the normalized daily CO<sub>2</sub> emissions ratios for Paris, Berlin, Munich, Amsterdam, Lyon, Marseille, and Nice in 2023. The y-axis represents each day's CO<sub>2</sub> emissions divided by the city's total emissions in 2023. These cities were selected due to the availability of corresponding Carbon Monitor Cities data (hereafter CM-Cities data, shown as green dashed lines), which enables direct comparison with the results of this study (blue lines). The time series data reveals distinct seasonal and weekly variations. The summer months (July and August) show a significant decline in emissions in Paris, Amsterdam, and Lyon, while emissions in all seven cities decline around Christmas, due to business closures and decreased commuting. For weekly patterns, there is a slight upward trend from Monday to Friday, a noticeable drop on Saturday, and a further decline on Sunday (Figure S6). The magnitude of the weekend drop varies across cities. In Berlin and Marseille, the median emissions on Sunday drop by approximately 31.1% and 27.7% compared to Friday in 2023, respectively, representing the most pronounced Sunday reduction among the six cities. In contrast, Amsterdam exhibits a much smaller Sunday drop compared to Friday (10.1%).

In all cities, the median emissions of public holidays (marked in grey shades) and school holidays (marked in light blue shades) are lower than those of weekdays in 2023. Across all six cities, the median emissions on public holidays and school holidays were consistently lower than weekday levels in 2023, indicating a general reduction in traffic-related CO<sub>2</sub> emissions during holiday periods. In Paris, public holiday emissions were exceptionally low, even lower than Sunday levels by 5.2%. The pattern is different in Marseille, Berlin, and Nice, as the median emissions on public holidays exceeded those on Saturdays by 24.4%, 11.0%, and 6.4%, respectively. The medians of school holidays are generally higher than those of public holidays because a more limited segment of the population is affected, and the distributions are notably wider. An exception is Amsterdam, where public holiday emissions slightly surpassed those during school holidays, suggesting a different urban rhythm or school break dynamics compared to other cities. Also, the day of the week on which a holiday falls also influences emission levels. As shown in Figure S7, holidays that coincide with weekends tend to show similar emission levels to regular weekend days. When holidays fall on a Monday, their emission levels are comparable to those of regular Mondays in cities like Berlin, Marseille, and Nice.

Although the general emission temporal variability estimated in this study align reasonably with those reported by Carbon Monitor Cities, as evidenced by the R correlation coefficients ranging from 0.58 to 0.84 across the six selected cities, notable differences remain. In Paris, CM-cities tends to underestimate both the troughs and peaks of emissions (Huo et al., 2022). In Lyon, the consistency is relatively high, but the sharp weekend emission drops observed in Carbon Monitor estimates are not reproduced in this study. In Amsterdam, this study does not show the pronounced weekend decreases during holidays that are present in Carbon Monitor data.

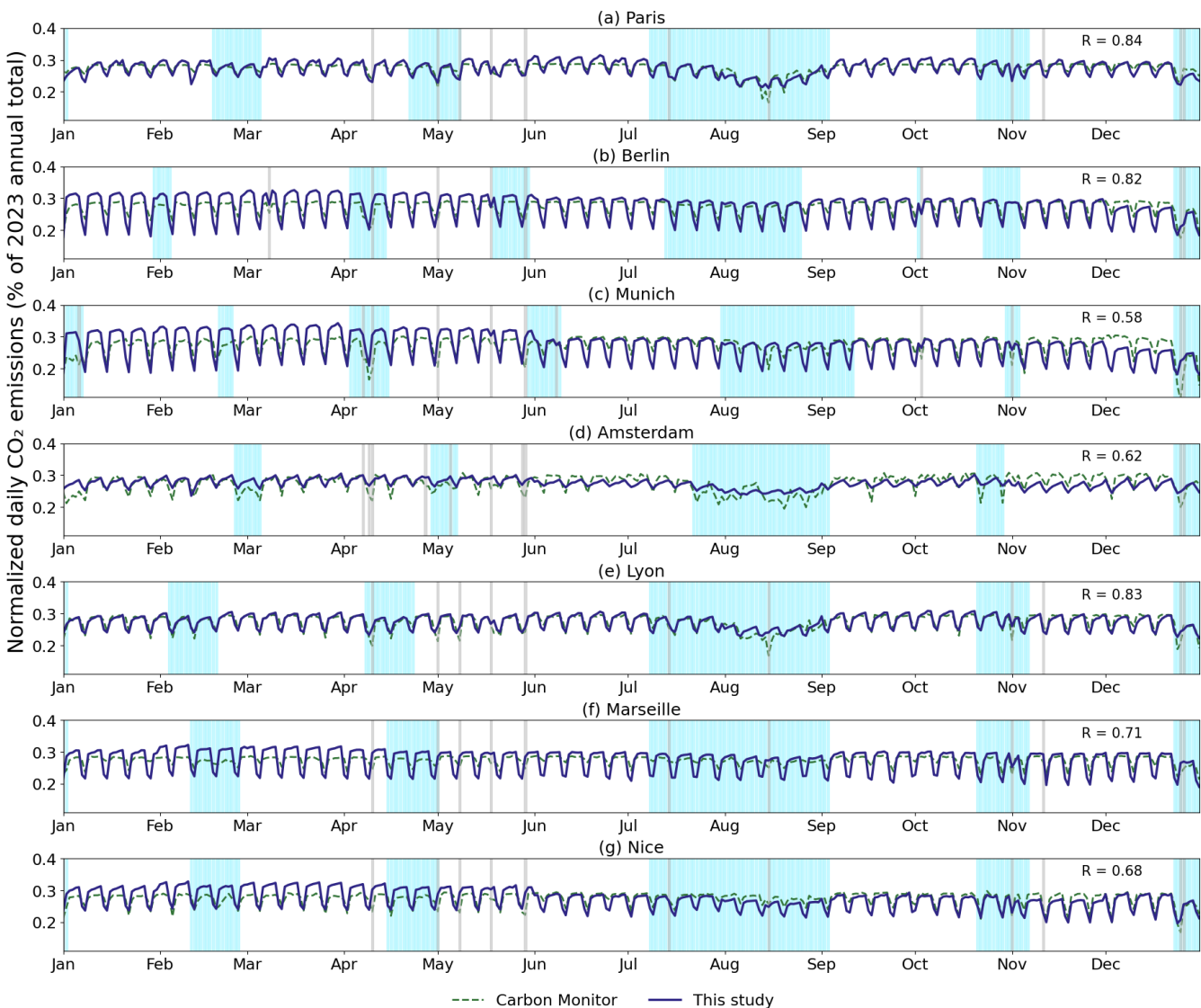


**Figure 6: Normalized daily CO<sub>2</sub> emission of seven cities in 2023.** Y-axis represents each day's CO<sub>2</sub> emissions divided by the city's total emissions in 2023. The light blue and grey shades represent school holidays and public holidays, respectively. The y-axis represents each day's CO<sub>2</sub> emissions divided by the city's total emissions in 2023.

Figure 7 presents the average hourly CO<sub>2</sub> emission patterns for cars across the 20 cities in 2023. The y-axis represents the average proportion of daily CO<sub>2</sub> emissions for each hour, categorized by day types: holidays (blue), weekdays (orange), and weekends (green). The hourly patterns for cars in French cities and Dutch cities are similar. On weekdays, there are two emission peaks at 9:00~10:00 and 18:00~19:00 due to commuting, and the emissions stabilize at relatively high levels between



these two peaks. After the second emission peak, the emissions decline continuously and reach their lowest point at 4:00 ~ 5:00. The differences between weekdays and holidays are relatively small, but with no or a less pronounced morning peak due to reduced commuting activity. On weekends, the sum of average emission share in French cities and Dutch cities during evening and early morning (22:00 to 6:00) reach 22.9% to 29.1%, significantly higher than that for weekdays (17.4 to 21.7%), and the first peak is lagged to around 12:00. German cities on weekdays, except for Dusseldorf, the CO<sub>2</sub> emission exhibit earlier morning peaks at 8:00 and a much higher peak around 15:00 ~16:00. On average, evening peak emissions in French and Dutch cities are only around 15% higher than morning peak levels, but for German cities specifically, the difference ranges from 9.3% to 60.0%. After the peak, the CO<sub>2</sub> emissions in German cities decrease sharply, which is consistent with the trends reported by the Berlin datasets (Max et al). On weekends, there is only one peak around 13:00.

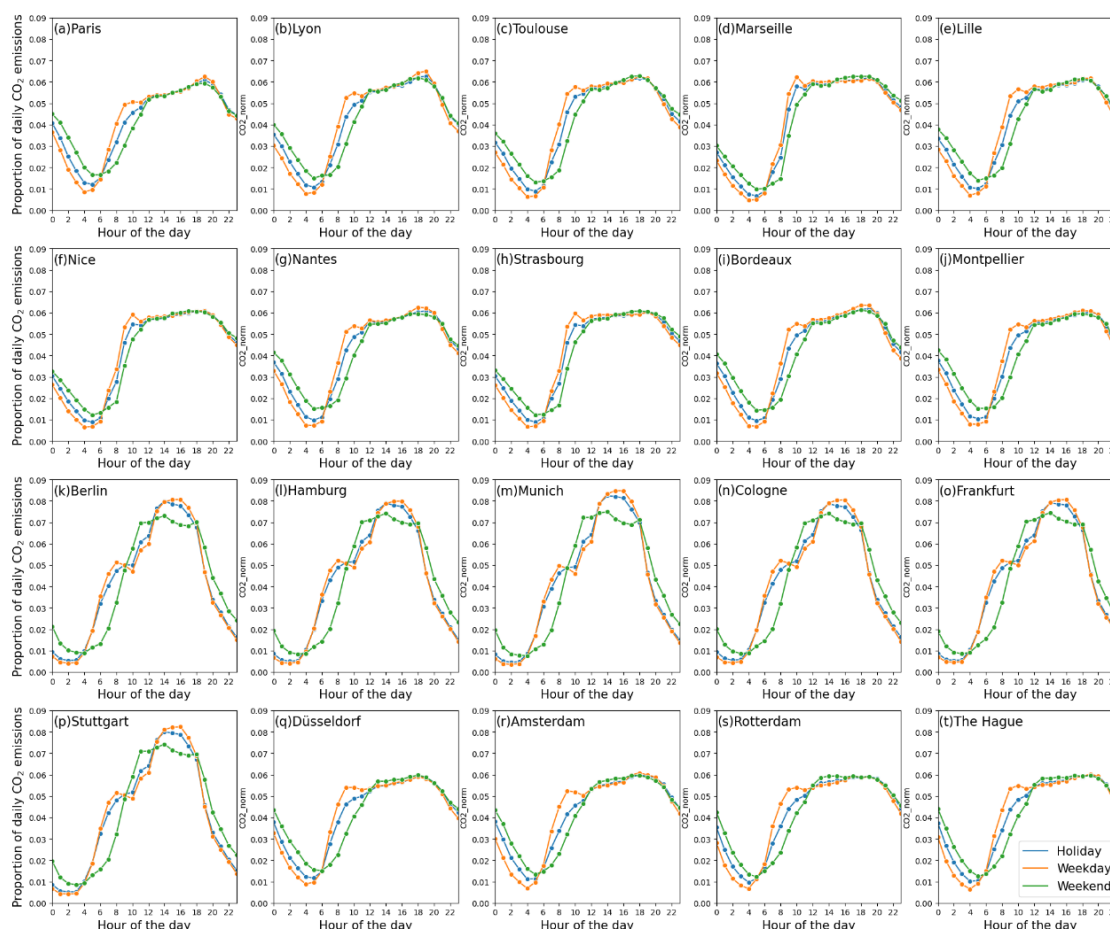


**Figure 7: Hourly emission patterns of cars in 20 cities.**

The hourly patterns for trucks are relatively consistent across all 20 European cities but are notably different from those of passenger cars (Figure 8). On weekdays, truck-related CO<sub>2</sub> emissions show a peak around 9:00 in nearly all cities, suggesting synchronized delivery and logistics activity. This peak accounts for 5.4%–6.5% of daily truck emissions in French and Dutch



cities, and up to 9% in German cities such as Berlin and Hamburg. Truck emissions on weekends and holidays are considerably reduced, with no discernible peaks in most cities. In some German cities (e.g., Stuttgart and Düsseldorf), truck emissions remain below 3% of daily total at any hour during holidays, reflecting stricter weekend freight regulations. In contrast, emissions levels of trucks remain relatively high on weekends, especially in southern cities like Marseille and Nice, where midday peaks surpass 0.06 of daily emissions and are comparable to weekday levels.

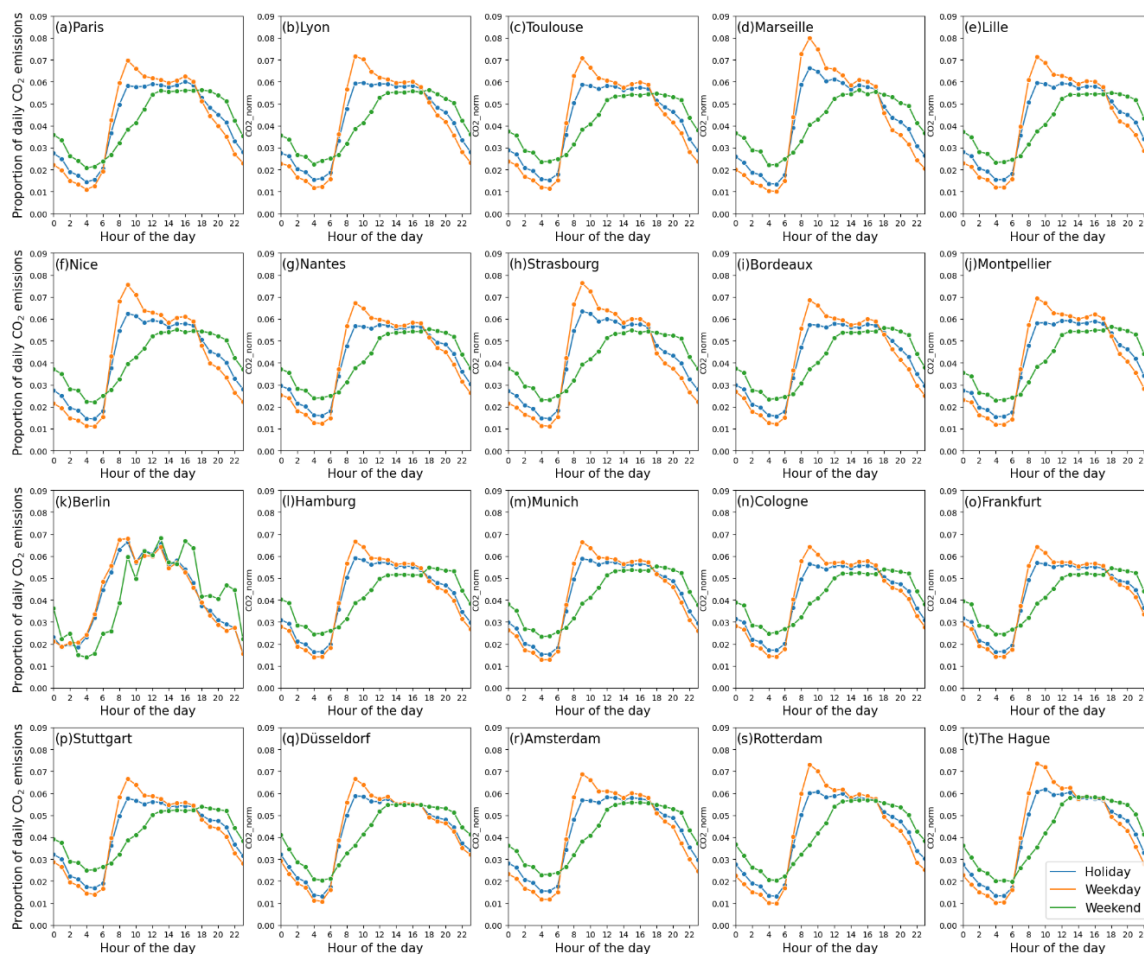


**Figure 8: Hourly emission patterns of trucks in 20 cities.**

### 3.4 Validation

Table S7 compares the annual emissions estimated in this study with those reported by Carbon Monitor and other available data sources. Carbon Monitor provides  $0.1^\circ \times 0.1^\circ$  daily gridded maps named GRACED (Dou et al., 2023). City boundaries were applied to clip GRACED grids, and area-weighted daily emissions were aggregated to annual city-level totals. Available



data of several cities from Climate Trace(Kott et al., 2024), local statistical websites(Bilanz des Statistikamtes Nord, 2024), and previous studies(Kühbacher et al., 2023; Ulrich et al., 2023; Anjos and Meier, 2025) was also collected. Overall, estimates of other datasets are much lower than this study, with differences ranging from  $-94.2\%$  (Nice, Carbon Monitor) to  $-8.1\%$  (Berlin, Ulrich et al.'s estimates from Opendata) relative to our estimates. These discrepancies can be explained by the methods of different datasets. Compared with local statistical reports, our estimates tend to be higher because we include emissions from vehicles traveling across city boundaries, whereas local statistics typically estimate emissions based only on oil consumption within administrative limits. GRACED allocates emissions based on EDGARv5 using OpenStreetMap data without actual traffic volume data, this method likely underestimates emissions in large cities with high-volume roads. Climate Trace estimates average annual daily traffic (AADT) by integrating Sentinel-2 satellite imagery with AADT data from the U.S. Department of Transportation's Federal Highway Administration (FHWA), applying Convolutional Neural Network and Graph Neural Network models. This U.S.-centric training may limit the models' applicability in the European context. Finally, although our approach benefits from a more comprehensive road network, the relatively low accuracy on middle and small roads may contribute to overestimation of traffic volumes in certain areas, as mentioned in Section 2.3.

For daily profiles, we have discussed the general consistencies and the notable differences between our estimates and those from CM-cities (Figure 6, Section 3.3). CM-cities estimated traffic volumes using a sigmoid regression based on TomTom live congestion indices, which lack spatial granularity (only one value per city), and the model parameters were calibrated using real-time data from approximately 60 roads in Paris. In addition, CM-cities adopts the Functional Urban Area (FUA) definition used by the OECD and the European Union, which includes high-density urban centers along with their surrounding commuting zones, whereas our analysis relies on administrative boundaries. For cities not covered by CM-cities, we compared daily emissions clipped from GRACED (Figure S8). Without calibration at the city level as CM-cities did, GRACED daily emissions fail to show a consistent weekday-weekend pattern, and some anomalous peaks occurred (e.g., elevated emissions in Hamburg in April 2023 and in Frankfurt and Montpellier in late May 2023). Except for The Hague, Rotterdam, and Bordeaux, the resulting daily profiles showed very poor agreement ( $R < 0.4$ ). These findings suggest that coarse-resolution data are not suitable for city-level temporal analyses, highlighting the advantage of our city-scale dataset in more accurately representing actual urban emissions.

## 4 Discussion

This study demonstrates that integrating new GPS-based traffic data for individual vehicles covering all street segments with the COPERT model enables the estimation of hourly on-road CO<sub>2</sub> emissions at street level, which were further aggregated into  $100 \times 100$  m grids for display purposes, to generate high-resolution emission maps across 20 European cities. This approach overcomes the limitations of traditional top-down downscaling methods (e.g., population-based or road-network density proxies) by applying machine learning to impute the actual traffic volumes from FCD, which only samples the traffic of



vehicles equipped with GPS. Compared to existing CO<sub>2</sub> emission inventories such as CAMS-TEMPO, Carbon Monitor, or localized platforms in Asian or German cities, our dataset represents a significant advancement by simultaneously achieving high spatial granularity and temporal resolution. It captures intra-urban variability that is often missed in coarser-resolution datasets or those relying solely on major road segments. This work highlights the value of integrating GPS-based mobility data with machine learning and emission modelling to enhance the monitoring of urban transportation emissions and to inform the design of effective, location-specific mitigation policies. Most recurrent low-carbon transport measures in cities include modal shift to public transport, low-carbon zones control, and low-emission vehicle development, but each strategy may vary according to development stages and types of urban land-use transport systems (Creutzig et al., 2012; Nakamura and Hayashi, 2013; Croci et al., 2021). While low-density cities become more compact in the long term but often lack sufficient population density to support rapid transit systems in the short term, promoting the adoption of electric vehicles, particularly in regions with low-carbon electricity, may be a more practical approach (Kennedy et al., 2014). This study may support the design of such strategies by enabling street-level scenarios to quantitatively assess their potential emission reductions.

Our CO<sub>2</sub> hourly emission maps reveal striking spatial heterogeneity within cities. For example, concentrated emission hotspots along Paris' ring road, versus more dispersed patterns in Berlin, reflect differences in urban structure, transport systems, and commuting behaviours. Temporally, we observed national variations in traffic-related emissions during holiday and summer periods, likely due to country-specific vacation schedules. Our new emission maps can support planning of low-emission zones, help identify high-flux corridors for targeted energy efficiency measures and provide a basis for congestion-related studies. Given that traffic congestion is a major driver of both fuel consumption and emissions, our maps offer valuable insights for designing and evaluating emission reduction strategies.

However, several sources of uncertainty remain in our approach, primarily stemming from the FCD. First, although we conducted extensive data cleaning, anomalies occasionally persist due to the instability and noise inherent in the raw data. Second, there are uncertainties related to the GPS penetration rate. The proportion of vehicles equipped with GPS devices may vary across vehicle types and cities. For instance, commercial vehicles are more likely to be tracked. This discrepancy may lead to bias in estimating traffic volume from floating car data (FCD), particularly if the raw data or sensor-based counts do not distinguish between vehicle categories. This study assumes that other cities have the same penetration rates as Paris or Berlin, but if the other cities have lower penetrations, then their traffic volumes are underestimated. In such cases, trucks may be overrepresented in the dataset, potentially leading to overestimation of freight-related emissions. Third, uncertainties also arise from fleet structures. Due to the lack of detailed vehicle-type distribution at the road segment level, we can only perform fleet correction for roads where heavy-duty vehicle traffic is explicitly restricted. For other roads, we currently apply city-wide average fleet compositions, which may not reflect local variations. Finally, significant errors may be introduced during the conversion from GPS trajectories to actual traffic volume. Our flux-to-volume machine learning models were calibrated using sensor data from Paris and Berlin only, as high-quality in-situ traffic observations are either unavailable or not publicly





accessible for other cities. As discussed in Section 3.4, the models for middle and small roads in Paris still require further refinement for better performance. This limits the models' generalizability and highlights the need for more comprehensive, standardized traffic monitoring networks. Some traffic data from other cities are available at daily or annual resolutions (Bonnemaizon et al., 2025), and integrating these in future work could support broader validation and model refinement. Also, the fleet captured by FCD and local monitoring stations can be different. For example, utility vehicles are captured by FCD but not by the Berlin Open Data traffic counts, which could be the reason for the bad performance when we try to transform signals to the real volumes for trucks. Incorporating additional top-down constraints, such as detailed fuel consumption data could potentially improve the accuracy of this step.

Current work only covers the year 2023, but the underlying GPS-based FCD is typically available with a delay of only about one week. This creates a clear opportunity to automate the processing pipeline and update the emission estimates on a rolling basis. Incorporating this capability into Carbon Monitor Cities would allow near-real-time, high-resolution emission monitoring at the street level, significantly enhancing the system's responsiveness and value for both research and policy applications. Also, future work could extend the methodology to include major air pollutants beyond CO<sub>2</sub>, and scale the approach to cover broader regions. Through incorporating more sensor-based traffic measurements across cities, data representativeness and model validation can be further improved. Such efforts will strengthen the robustness, applicability, and policy relevance of street-level emission mapping, particularly in supporting timely decision-making and climate or clean air action monitoring.

## 5 Data availability

The high-resolution hourly CO<sub>2</sub> emission dataset for 20 cities in 2023 is available in NetCDF format, on Zenodo <https://doi.org/10.5281/zenodo.16600210> (Shi et al., 2025). Each city has an individual NetCDF file that provides gridded hourly emissions over the entire year of 2023. Their central x and y coordinates define the grid cells, and each file includes the variable CO2\_g, representing emissions in grams per hour in the grid. Every grid's size is 100 m × 100 m.

## Supplement

This dataset is accompanied by Supplementary Information, including a detailed methodology document (SI\_document.docx) and additional data tables (SI\_tables.xlsx).





## Author contributions

QS processed and generated the dataset and drafted the initial manuscript. PC designed the study and provided scientific supervision. NM collected the raw data and contributed to the structuring of the dataset. XB and RTM assisted with COPERT data handling, data matching, and emission calculations. RE reviewed the emission estimates and provided constructive feedback on the manuscript. CZ contributed extensively to the machine learning modelling and provided valuable suggestions on the manuscript structure and visualization. All authors reviewed and approved the final manuscript.

## Competing interests

The authors declare that they have no conflict of interest.

## Acknowledgement

This study is funded by the Copernicus Atmosphere Monitoring Service (under the CAMS2\_51a contract), which is implemented by the European Centre for Medium-Range Weather Forecasts (ECMWF) on behalf of the European Commission.

## References

- Albarus, I., Lauvaux, T., Utard, H., Ciais, P., Crifo, P., and Gros, V.: Unraveling climate targets across the Paris conurbation as a gauge of city ambitions, *npj Urban Sustainability*, 5, 27, 10.1038/s42949-025-00206-y, 2025.
- Amsterdam, T. C. o.: Roadmap Amsterdam Climate Neutral 2050, 2024.
- Anjos, M. and Meier, F.: Zooming into Berlin: tracking street-scale CO<sub>2</sub> emissions based on high-resolution traffic modeling using machine learning, *Frontiers in Environmental Science*, 12, 10.3389/fenvs.2024.1461656, 2025.
- Verkehrsdetektion Berlin: <https://daten.berlin.de/datensaetze/verkehrsdetektion-berlin>, last access: 28/07/2025.
- Erneut deutliche CO<sub>2</sub>-Minderung in Hamburg: <https://www.hamburg.de/politik-und-verwaltung/behoerden/bukea/themen/klima/klimaschutz-klimaplan/co2-bilanz-hh-2023-169240>, last access: 28/07/2025.
- Bonnemaizon, X., Ciais, P., Zhou, C., Shi, Q., Mittakola, R. T., Goldmann, C., Ben Arous, S., Megel, N., and Davis, S. J.: Harmonized Annual Averaged Traffic Data at Street Segment Level for European Cities, *Scientific Data*, 12, 1365, 10.1038/s41597-025-05698-y, 2025.
- E-Mobility revolution in Amsterdam: [https://cinea.ec.europa.eu/news-events/news/e-mobility-revolution-amsterdam-2025-04-23\\_en?utm\\_source=chatgpt.com](https://cinea.ec.europa.eu/news-events/news/e-mobility-revolution-amsterdam-2025-04-23_en?utm_source=chatgpt.com), last access: 28/07/2025.
- Creutzig, F., Mühlhoff, R., and Römer, J.: Decarbonizing urban transport in European cities: four cases show possibly high co-benefits, *Environmental research letters*, 7, 044042, 2012.
- Croci, E., Lucchitta, B., and Molteni, T.: Low carbon urban strategies: An investigation of 124 European cities, *Urban Climate*, 40, 101022, <https://doi.org/10.1016/j.uclim.2021.101022>, 2021.
- De Gennaro, M., Paffumi, E., and Martini, G.: Big Data for Supporting Low-Carbon Road Transport Policies in Europe: Applications, Challenges and Opportunities, *Big Data Research*, 6, 11-25, <https://doi.org/10.1016/j.bdr.2016.04.003>, 2016.
- Field of Action: Transport: [https://dibek.berlin.de/?lang=en#caption\\_c2c12](https://dibek.berlin.de/?lang=en#caption_c2c12), last access: 28/07/2025.
- Dou, X., Hong, J., Ciais, P., Chevallier, F., Yan, F., Yu, Y., Hu, Y., Huo, D., Sun, Y., Wang, Y., Davis, S. J., Crippa, M., Janssens-Maenhout, G., Guizzardi, D., Solazzo, E., Lin, X., Song, X., Zhu, B., Cui, D., Ke, P., Wang, H., Zhou, W., Huang, X., Deng, Z., and Liu, Z.: Near-real-time global gridded daily CO<sub>2</sub> emissions 2021, *Scientific Data*, 10, 69, 10.1038/s41597-023-01963-0, 2023.



EEA greenhouse gases — data viewer: <https://www.eea.europa.eu/en/analysis/maps-and-charts/greenhouse-gases-viewer-data-viewers?activeTab=570bee2d-1316-48cf-adde-4b640f92119b>, last access: 28/07/2025.

Greenhouse gas emissions from transport in Europe: <https://www.eea.europa.eu/en/analysis/indicators/greenhouse-gas-emissions-from-transport?activeAccordion=309c5ef9-de09-4759-bc02-802370dfa366>, last access: 28/07/2025.

Gately, C. K., Hutyrá, L. R., and Sue Wing, I.: Cities, traffic, and CO<sub>2</sub>: A multidecadal assessment of trends, drivers, and scaling relationships, *Proc Natl Acad Sci U S A*, 112, 4999–5004, 10.1073/pnas.1421723112, 2015.

Guevara, M., Jorba, O., Tena, C., Denier van der Gon, H., Kuenen, J., Elguindi, N., Darras, S., Granier, C., and Pérez García-Pando, C.: Copernicus Atmosphere Monitoring Service TEMPoral profiles (CAMS-TEMPO): global and European emission temporal profile maps for atmospheric chemistry modelling, *Earth Syst. Sci. Data*, 13, 367–404, 10.5194/essd-13-367-2021, 2021.

Huo, D., Huang, X., Dou, X., Ciais, P., Li, Y., Deng, Z., Wang, Y., Cui, D., Benkhelifa, F., Sun, T., Zhu, B., Roest, G., Gurney, K. R., Ke, P., Guo, R., Lu, C., Lin, X., Lovell, A., Appleby, K., DeCola, P. L., Davis, S. J., and Liu, Z.: Carbon Monitor Cities near-real-time daily estimates of CO<sub>2</sub> emissions from 1500 cities worldwide, *Scientific Data*, 9, 533, 10.1038/s41597-022-01657-z, 2022.

Tomtom traffic index: <https://www.tomtom.com/traffic-index/about/>, last access: 28/07/2025.

Kennedy, C. A., Ibrahim, N., and Hoorweg, D.: Low-carbon infrastructure strategies for cities, *Nature Climate Change*, 4, 343–346, 10.1038/nclimate2160, 2014.

Transportation Sector - Global Road Emissions, Climate TRACE Emissions Inventory: <https://unfccc.int/climate-action/un-global-climate-action-awards/climate-leaders/city-of-paris>, last access: 28/07/2025.

Kühbacher, D., Aigner, P., Super, I., Droste, A., Denier van der Gon, H., Ilic, M., and Chen, J.: Bottom-up estimation of traffic emissions in Munich based on macroscopic traffic simulation and counting data, EGU General Assembly 2023, Vienna, Austria, <https://doi.org/10.5194/egusphere-egu23-12997>, 2023.

Naiudomthum, S., Winijkul, E., and Sirisubtawee, S.: Near Real-Time Spatial and Temporal Distribution of Traffic Emissions in Bangkok Using Google Maps Application Program Interface, 10.3390/atmos13111803, 2022.

Nakamura, K. and Hayashi, Y.: Strategies and instruments for low-carbon urban transport: An international review on trends and effects, *Transport Policy*, 29, 264–274, <https://doi.org/10.1016/j.tranpol.2012.07.003>, 2013.

Ntziachristos, L., Gkatzoflias, D., Kouridis, C., and Samaras, Z.: COPERT: a European road transport emission inventory model, *Information Technologies in Environmental Engineering: Proceedings of the 4th International ICSC Symposium Thessaloniki, Greece, May 28–29, 2009*, 491–504,

Comptage routier - Données trafic issues des capteurs permanents: [https://opendata.paris.fr/explore/dataset/comptages-routiers-permanents/information/?disjunctive.libelle&disjunctive.libelle\\_nd\\_ament&disjunctive.libelle\\_nd\\_aval&disjunctive.etat\\_trafic](https://opendata.paris.fr/explore/dataset/comptages-routiers-permanents/information/?disjunctive.libelle&disjunctive.libelle_nd_ament&disjunctive.libelle_nd_aval&disjunctive.etat_trafic), last access: 28/07/2025.

An introduction to explainable AI with Shapley values: [https://shap.readthedocs.io/en/latest/example\\_notebooks/overviews/An%20introduction%20to%20explainable%20AI%20with%20Shapley%20values.html](https://shap.readthedocs.io/en/latest/example_notebooks/overviews/An%20introduction%20to%20explainable%20AI%20with%20Shapley%20values.html), last access: 28/07/2025.

Shi, Q., Ciais, P., Megel, N., Bonnemaizon, X., Mittakola, R. T., Engelen, R., and Zhou, C.: High spatiotemporal resolution traffic CO<sub>2</sub> emission maps derived from Floating Car Data (FCD) for 20 European cities (2023), Zenodo [dataset], 10.5281/zenodo.16600210, 2025.

Ulrich, V., Brückner, J., Schultz, M., Vardag, S. N., Ludwig, C., Fürle, J., Zia, M., Lautenbach, S., and Zipf, A.: Private Vehicles Greenhouse Gas Emission Estimation at Street Level for Berlin Based on Open Data, *ISPRS International Journal of Geo-Information*, 12, 138, 2023.

City of Paris: Carbon Neutral by 2050 for a Fair, Inclusive and Resilient Transition | France: <https://unfccc.int/climate-action/un-global-climate-action-awards/climate-leaders/city-of-paris>, last access: 28/07/2025.

Wen, Y., Wu, R., Zhou, Z., Zhang, S., Yang, S., Wallington, T. J., Shen, W., Tan, Q., Deng, Y., and Wu, Y.: A data-driven method of traffic emissions mapping with land use random forest models, *Applied Energy*, 305, 10.1016/j.apenergy.2021.117916, 2022.

Xavier Bonnemaizon, P. C., Chuanlong Zhou, Simon Ben-Arous, Steven J Davis, Nicolas Megel: Scaling traffic variables from sensors sample to the entire city at high spatiotemporal resolution with machine learning: applications to the Paris megacity, <https://eartharxiv.org/repository/view/6948/>, 2024.